VOL. 82, NO. 17 GL02717 JOURNAL OF GEOPHYSICAL RESEARCH JUNE 10, 1977

FC
AREA
ID
SRP
MT

Geothermal Significance of Magnetotelluric Sounding in the Eastern Snake River Plain–Yellowstone Region

W. D. Stanley

U.S. Geological Survey, Denver, Colorado 80225

J. E. Boehl, F. X. Bostick, and H. W. Smith

University of Texas at Austin, Austin, Texas 78712

Magnetotelluric soundings along a profile extending from the Raft River geothermal area in southern Idaho to Yellowstone National Park in Wyoming reveal a highly anomalous crustal structure involving a conductive zone at depths that range from 18 km in the central part of the eastern Snake River Plain to 7 km beneath the Raft River thermal area and as little as 5 km in Yellowstone. Resistivities in this conductive zone are less than 10 ohm m and at some sites less than 1 ohm m. Structural parameters obtained in processing the magnetotelluric data suggest the possibility of a conductive axis along the center of the eastern Snake River Plain, and these parameters also point to very conductive structures beneath the Yellowstone caldera system. A sounding completed in the Island Park caldera can only be modeled with a crustal structure very different from the Yellowstone caldera system, requiring the absence of this conductive zone to depths greater than 25 km in the Island Park caldera. In addition to the deep conductive zone the thickness of extensive surface basalts in the eastern Snake River Plain was mapped geophysically, and units between the basalts and the deep conductive zone were also well defined and fitted to geologic models.

Introduction

The Snake River Plain is one of the most striking and enigmatic geologic features in the western United States. The plain is an arcuate depression of very low relief that contrasts with the surrounding mountainous topography. It extends for more than 500 km across southern Idaho (Figure 1). Much of the plain is underlain by basalt and interbedded continental sediments of the Quaternary Snake River Group and the Quaternary and Tertiary Idaho Group that dip gently, generally toward its central axis. Both faulting and downwarping appear to have contributed to the subsidence of the region. The structure of the western part of the Snake River Plain is grabenlike, bounded on the north by northwest trending en echelon normal faults [*Malde*, 1959]. The eastern part of the Snake River Plain, however, appears to have been downwarped to a greater extent [*McIntyre*, 1972]. Most of the volcanic rocks of the Snake River Plain are of Miocene and younger ages ranging from 20 m.y. to the very recent flows at Craters of the Moon, which have been dated at 2100 yr [*Bullard*, 1971]. These volcanic rocks form a bimodal suite of basalt and rhyolite commonly associated with mantle-generated magmas. The structural grain produced during late Mesozoic compressional mountain building and Cenozoic block faulting, the latter being related to crustal extension of the Basin and Range province, is approximately northwest, nearly perpendicular to the axis of the eastern Snake River Plain. Where older structures plunge under the plain, they are not deflected or offset in any way that would suggest that the Snake River downwarp was a significant tectonic feature before Miocene time.

The Yellowstone and Island Park rhyolite plateau has been the scene of three cycles of Quarternary volcanism, each of which was climaxed by a devastating pyroclastic eruption of enormous rhyolite ash flows and collapse of the volcanic source area to form a large caldera [*Christiansen and Blank*, 1972]. Basalts and rhyolites were erupted during each cycle; the rhyolites overwhelmingly predominate. Rocks of intermediate composition are virtually absent. The oldest cycle climaxed about 1.9 m.y. ago, forming a caldera complex that extended from Island Park to perhaps the central part of Yellowstone. The second cycle was confined to the Island Park area and climaxed about 1.2 m.y. ago. The third cycle formed most of the present-day rhyolite plateau in Yellowstone and began about 1.6 m.y. ago, the most recent activity being between 150,000 and 70,000 yr ago. Doming of the western part of the Yellowstone caldera system as recently as 150,000 yr ago probably indicates a new magmatic insurgence, and it is thought that the present very active and hot hydrothermal systems probably all date from this insurgence [*Eaton et al.*, 1975].

Additional interest has been focused on the Snake River Plain–Yellowstone region because of its potential for geothermal power. Yellowstone, of course, is the most dramatic thermal manifestation in the United States, and several million dollars have been spent on exploration and development of a hot water geothermal system near Raft River, Idaho [*Williams et al.*, 1975] (Figure 1). Other geothermal areas have been located at Bruneau-Grandview and in the Weiser area in the western part of the Snake River Plain. The study described in this paper was designed to provide some insight into the overall geothermal potential of the Snake River Plain–Yellowstone region through a study of the crustal electrical properties of the area down to depths of about 20 km. Previous electrical studies have been made in the Snake River Plain by *Zohdy and Stanley* [1973], *Jackson* [1974], and *Leary and Phinney* [1975]. Long-line refraction studies have been made by *Hill and Pakiser* [1966], and extensive gravity surveys have been completed by *Mabey* [1975], *Hill* [1963], and *Bonini* [1963]. Shallow electrical studies have been made in Yellowstone by *Zohdy et al.* [1973]; extensive gravity, magnetic, microearthquake, and teleseismic delay studies are described by *Eaton et al.* [1975]; *Bhattacharyya and Leu* [1975] and *Smith et al.* [1974] have computed Curie point depths for the Yellowstone area; and *Iyer* [1975] has studied seismic noise in Yellowstone geyser

Paper number 7B0117.

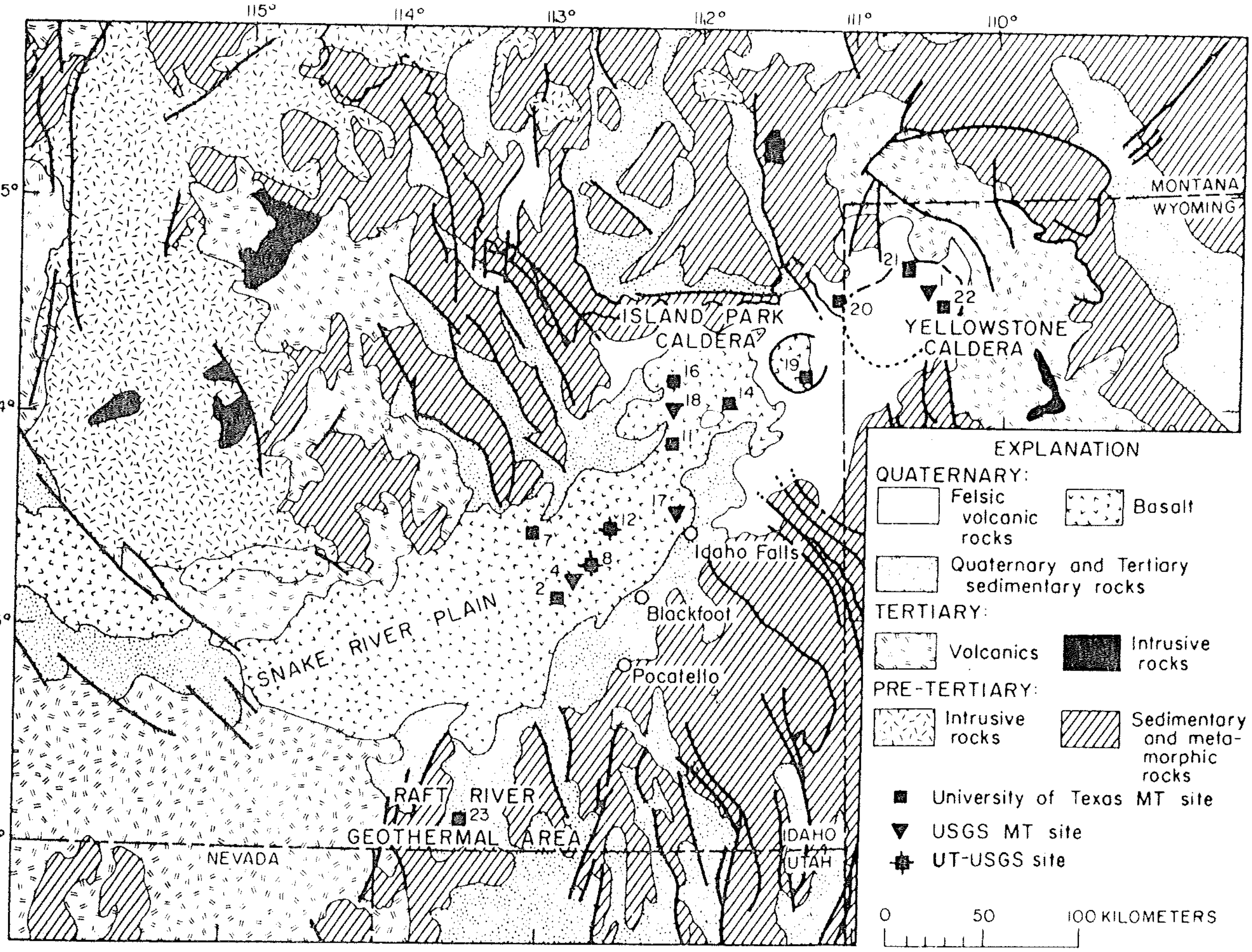

Fig. 1. Generalized geologic map and location of MT sites. Geology and base from National Geologic Map, western half, USGS, 1975.

basins. Extensive geophysical studies have been made of the Raft River geothermal area by the U.S. Geological Survey (USGS) [*Williams et al.*, 1975], and *Long* [1977] has made electrical studies in the Island Park caldera.

Survey Design

Magnetotelluric (MT) soundings were used to study crustal electrical structure down to depths of at least 20 km. Three recording systems were used at various times during the survey. The prime system consisted of an MT-AMT (magnetotelluric-audiomagnetotelluric) system built and operated by the University of Texas (UT) Geomagnetics Laboratory. Data from this system formed the main core of the data for the survey. In addition, a low-frequency system using coils similar to the UT system was operated at base stations along the survey profile to acquire data simultaneously with the prime system. These simultaneous station data will be used in an attempt to investigate source field behavior; however, the study is not yet complete and will be the subject of a subsequent report. Also, a digital cryogenic magnetometer MT system being developed by the USGS was used to obtain data at five sites in the survey area. Problems with magnetometer dewars and electronic problems prevented the occupation of more than five sites with the cryogenic system. The design of this cryogenic MT system will also be described in a subsequent paper.

Magnetotelluric Principles

The scalar MT method as described by *Cagnaird* [1953] is adequate for a layered earth but may give grossly distorted results in regions where the earth has a more complicated structure. An impedance tensor model [*Cantwell*, 1960; *Bostick and Smith*, 1962; *Swift*, 1967] is more representative of most situations, since it does permit two-dimensional geometry. The tensor relations between E and H fields may be derived from Maxwell's equations and expressed as

$$[E] = [Z][H] \tag{1}$$

or

$$E_x = Z_{xx}H_x + Z_{xy}H_y \qquad E_y = Z_{yx}H_x + Z_{yy}H_y \tag{2}$$

where the impedance tensor is

$$[Z] = \begin{bmatrix} Z_{xx} & Z_{xy} \\ Z_{yx} & Z_{yy} \end{bmatrix} \tag{3}$$

For two-dimensional geometries the principal impedance values Z_{xy}' and Z_{yx}' are calculated with axes parallel and perpendicular to the strike of the two-dimensional inhomogeneity. If the data appear to indicate three-dimensional qualities, the same procedure is used in an attempt to extract a two-dimensional fit from the results.

Instead of the impedance tensor being rotated to the principal axes [*Sims and Bostick*, 1969], the electric and magnetic field data are projected onto the rotated axes, and then the tensor estimates are computed. This procedure allows the calculation of the coherencies associated with the principal impedance values. The rotation angle ϕ, which maximizes $|Z_{xy}|^2 + |Z_{yx}|^2$, locates the principal axes and for two-dimensional situations requires Z_{xx}' and Z_{yy}' to be zero. In this case the tensor decouples into two modes represented by

$$E_x' = Z_{xy}' H_y' \qquad E_y' = Z_{yx}' H_x' \tag{4}$$

From the principal impedance values the principal resistivity values are computed as

$$\rho_{xy}' = (0.2/f)\,|Z_{xy}'|^2 \qquad \rho_{yx}' = (0.2/f)\,|Z_{yx}'|^2 \tag{5}$$

where f is the frequency; one of these values is a maximum, and the other is a minimum.

Also associated with the principal impedances are the respective phases

$$\varphi_{yx}' = \tan^{-1} X_{yx}'/R_{yx}' \qquad \varphi_{xy}' = \tan^{-1} X_{xy}'/R_{xy}'$$

where R and X are the real and imaginary parts, respectively, of Z.

One common procedure in MT interpretation is to perform one-dimensional inversions of (5) to produce resistivity versus depth profiles. A number of methods have been used for the one-dimensional inversion [*Wu*, 1968; *Patrick and Bostick*, 1969; *Becher and Sharpe*, 1969; *Greenfield and Turnbull*, 1970; *Laird and Bostick*, 1970; *Johnson and Smylie*, 1970]. Finite difference methods have also been used for the inversion of MT data for two-dimensional models by *Swift* [1967] and *Patrick and Bostick* [1969].

DATA ACQUISITION

Figure 1 indicates the location of 16 MT sites occupied in the survey of the eastern Snake River Plain–Yellowstone region. At each of the sites, tensor impedance estimates were obtained through broadband measurements of the five components (E_x, E_y, H_x, H_y, and H_z) of surface electric and magnetic fields of the earth. The UT recording system was used at 12 of the sites shown in Figure 1, and the USGS cryogenic system was used at 5 sites. For the 12 UT sites a low-frequency band of 0.001–1 Hz and a midfrequency band of 0.05–10 Hz were used. Systems filters were adjusted to provide approximately prewhitened data throughout these bands, and the results were recorded on FM tape. At each site, 4 hours of recording time were required for the low band, whereas 1.5 hours of data were taken for the midband. A high-frequency band of data from 1 Hz to over 1 KHz was acquired through the AMT part of the UT system. This system consists of a set of preamps and prefilters followed by a tuneable double-conversion superheterodyne phase sensitive receiver. The data analysis portion of the AMT system is implemented through a programable calculator, which provided preliminary real time results while the equipment was on site. Initial results, including autospectral and cross-spectral estimates as well as impedances, coherencies, etc., were recorded on magnetic cards on the calculator system.

Recording at the USGS sites with the cryogenic system consisted of digital (12-bit resolution) recording over a single flat band from dc to 0.5 Hz, the only filtering being for 60- to 180-Hz rejection and antialiasing. Four hours of data at a 1-s sample interval typically were recorded in a single span with the USGS system, but electronic problems recurring throughout the survey allowed the use of only about 50% of the data.

DATA ANALYSIS

The low-band data from the UT system and the data from the USGS system were processed in a similar manner, although different computer programs were used in each instance. The only significant difference in processing was that the broadband data from the USGS system was digitally prewhitened and used an optimum smoothing window designed to minimize spectral leakage [*Otnes and Enochson*, 1972], which was more severe with the dc response of the cryogenic magnetometer. A multichannel time series, typically 4096 points in length, was spectrally decomposed by using a fast Fourier transform algorithm, and harmonics were averaged over constant bandwidth intervals. The spectra were rotated to the direction of principal axes parallel and perpendicular to the strike of the two-dimensional inhomogeneity [*Word et al.*, 1970]. The principal impedance value in which the electric field is parallel to the two-dimensional structure, called $E_\parallel$ or TE (transverse electric), was determined from testing for maximum coherency between H_x and H_z.

Data for the midfrequency band of the UT system were analyzed by replaying the analog FM data into the AMT receiver. The required frequency multiplication was accomplished by varying the tape replay speed. The resulting spectral outputs of the receiver were rotated to the principal axes mathematically, the tensor impedances calculated, and the $E_\parallel$ or TE impedance determined.

Ideally, the inversion of MT data requires a smoothly varying function of apparent resistivity versus frequency. Any noise encountered in the measurement or analysis process results in scattered points when the apparent resistivities are calculated. For some magnetotelluric inversion techniques this scatter is not a serious problem, but for the 'continuous'

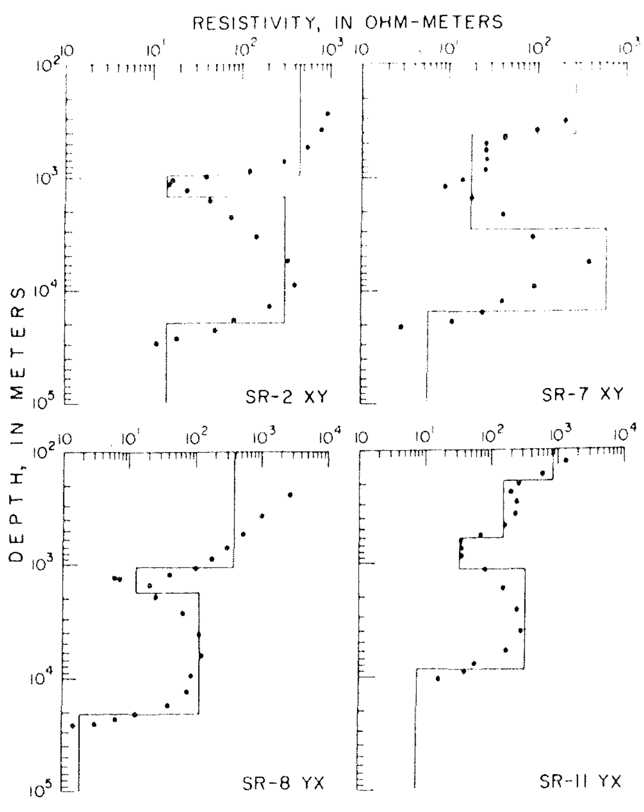

Fig. 2. 'Continuous' and simplified layered models for MT soundings 2, 7, 8, and 11.

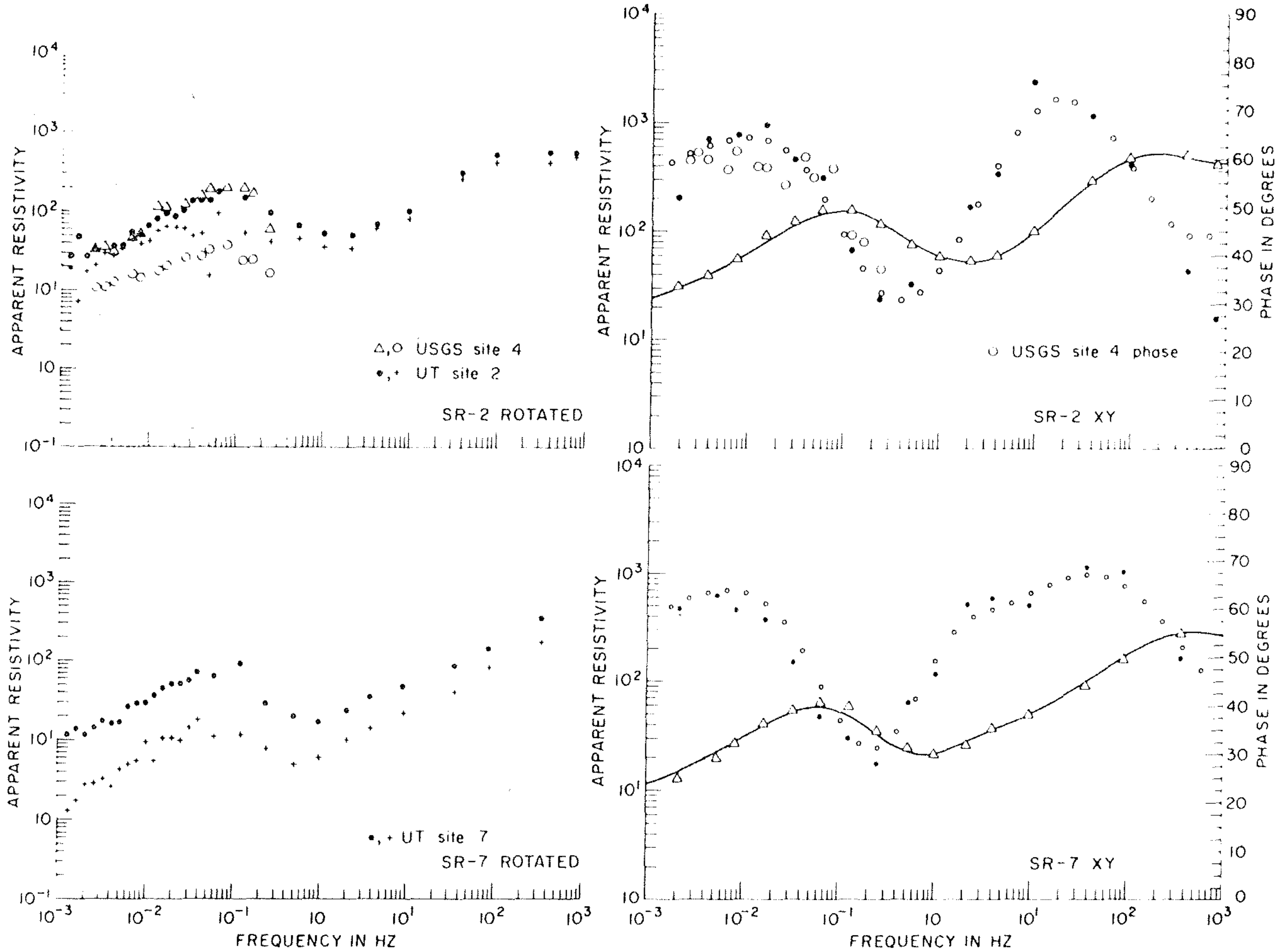

Fig. 3. MT data from UT sites 2 and 7. On the left are shown the tensor resistivity amplitudes, and on the right are the resistivity phase for the TE direction (solid circles), phase-derived amplitude curves for the TE direction (triangles or squares), and computed phase and amplitude (open circles and solid lines, respectively). Data from USGS site 4 are plotted on UT site 2 data.

inversion program used for 'first cut models' in this analysis, smooth apparent resistivity curves were necessary. An analytical technique was developed to perform the smoothing of the composite impedance curves obtained from the three frequency bands for the UT sites. This technique assumes that the magnetotelluric impedances along the principal axes are minimum phase functions [*Oppenheim and Schafer*, 1975], and amplitudes and phase on log-log plots versus frequency are related through Hilbert transform pairs. Smoothing is accomplished by deriving the log amplitude of the resistivity by numerically integrating the phase with weighting determined by coherencies. Techniques for doing this will be described along with the 'continuous' inversion program in a subsequent paper.

A layered model was established for most of the sites by a two-step inversion process. Initially, the 'continuous' inversion program, which computes a model layer for each frequency point, was applied to arrive at a model which could be simplified. The simplified model was obtained by reducing the number of layers to be used as a starting model for a generalized nonlinear inversion program [*Patrick and Bostick*, 1969; *Laird and Bostick*, 1970; B. D. Smith, written communication, 1975], which fits a layered model to the data in a least squares sense. The nonlinear inversion program was constrained to provide a model of not more than five layers at each MT site. Examples of 'continuous' inversions are shown in Figure 2 for sites 2, 7, 8, and 11. Models derived from this process are tabulated in Table 1. The MT data used to derive the models of Table 1 are shown in Figures 3–8. In the left part of each of the figures, resistivity amplitude curves for the rotated tensors are shown, and in the right part of the figures, several variables are plotted: (1) the phase-derived TE direction amplitude curves, shown by triangles or squares, (2) the observed phase curve for the TE direction, shown by solid circles, and (3) TE amplitude and phase curves calculated from the layered inversion models in Table 1, shown by solid lines and open circles, respectively. Results from the USGS sites are shown where the data were useable, namely, at sites 4, 8, 12, 17, and 1. USGS site 4 is shown in Figure 3 with UT site 2; data from USGS site 8 are shown at the identical UT site 8; data from USGS site 12 are shown at UT site 12; data from USGS site 17 are shown at UT site 11; and data from USGS site 1 are shown in Figure 7 with data from UT site 21. The data from USGS and UT sites 8 and 12 were not recorded simultaneously and were processed by using slightly different computer programs. Generally, the data agree, with the exception of a more pronounced maximum in the USGS site 12 TM data. Only one set of data was used in spectral processing of the USGS data; had more data been available, the two sets might have been closer in agreement.

GEOELECTRICAL CROSS SECTION

The models obtained in the inversion process were used to construct a geoelectrical cross section extending from the Raft River geothermal area to Yellowstone along the axis of the Snake River Plain. This cross section is shown in Figure 9 with vertical exaggerations of 10 to 1 and 1 to 1. Interpreted resistivities from the inversion process are shown in each layer beneath the sounding sites. The lowermost layer was indeterminate in thickness from the sounding data, which only extended to 0.001 Hz in frequency. We have labeled some of the layers with their probable geologic significance where such a relation seemed to exist. The resistive layer of several hundred ohm meters detected at sites 2, 4, 8, 12, 14, and 10 is assumed to be mostly a sequence of Snake River basalts of Quaternary age (Figure 1). Previous work with direct current soundings [*Zohdy and Stanley,* 1973] suggests that the resistivities of dry basalt (water table is generally at about 150 m or greater) is 500–1500 ohm m, and the resistivities of the fresh-water-saturated basalt in this area are 250–500 ohm m; therefore these results agree with the MT results. Even though we have interpreted this layer to be composed of basalts, in some locations, particularly from sites 14 to 19, geologic evidence suggests that rhyolites may be interbedded with the basalts. A conductive layer of 12–20 ohm m detected beneath the basalts at the previously mentioned stations, and at site 23 where there are no basalts, probably consists of a complex of basalts, rhyolite flows, welded tuffs, and sediments. The resistivities of 12–15 ohm m are similar to values observed for similar volcanic and sediment complexes in the Long Valley caldera, California [*Stanley et al.,* 1976].

The resistive layer, or third layer down on most of the soundings, is believed to represent both the basement complex of older sedimentary and metamorphic rocks and the granitic crust. The interpreted resistivities for this layer cannot be considered to be determined as accurately as the layers above or the conductive layer beneath. This limitation arises because of the difficulty in determining the true resistivity of a resistive layer with the MT method, unless the layer is at the surface. However, the resistivities are determined accurately enough so that we can state that the rather systematic decrease in third-layer resistivities from sites 2–14 does appear to be real. More will be said about this variation later.

The most significant feature of the model cross section is the lowermost conductive layer that was detected on all the soundings except possibly at site 19 in Island Park. The interpreted resistivities shown should not be considered highly accurate. For sites 1, 20, 21, 22, and 23 the conductive layer resistivity is about 1 ohm m or less, but for the rest of the soundings in the Snake River Plain the true resistivity is only known to be less than 10 ohm m. The lowest resistivities for this layer appear to be at the Raft River and Yellowstone sites, and the highest

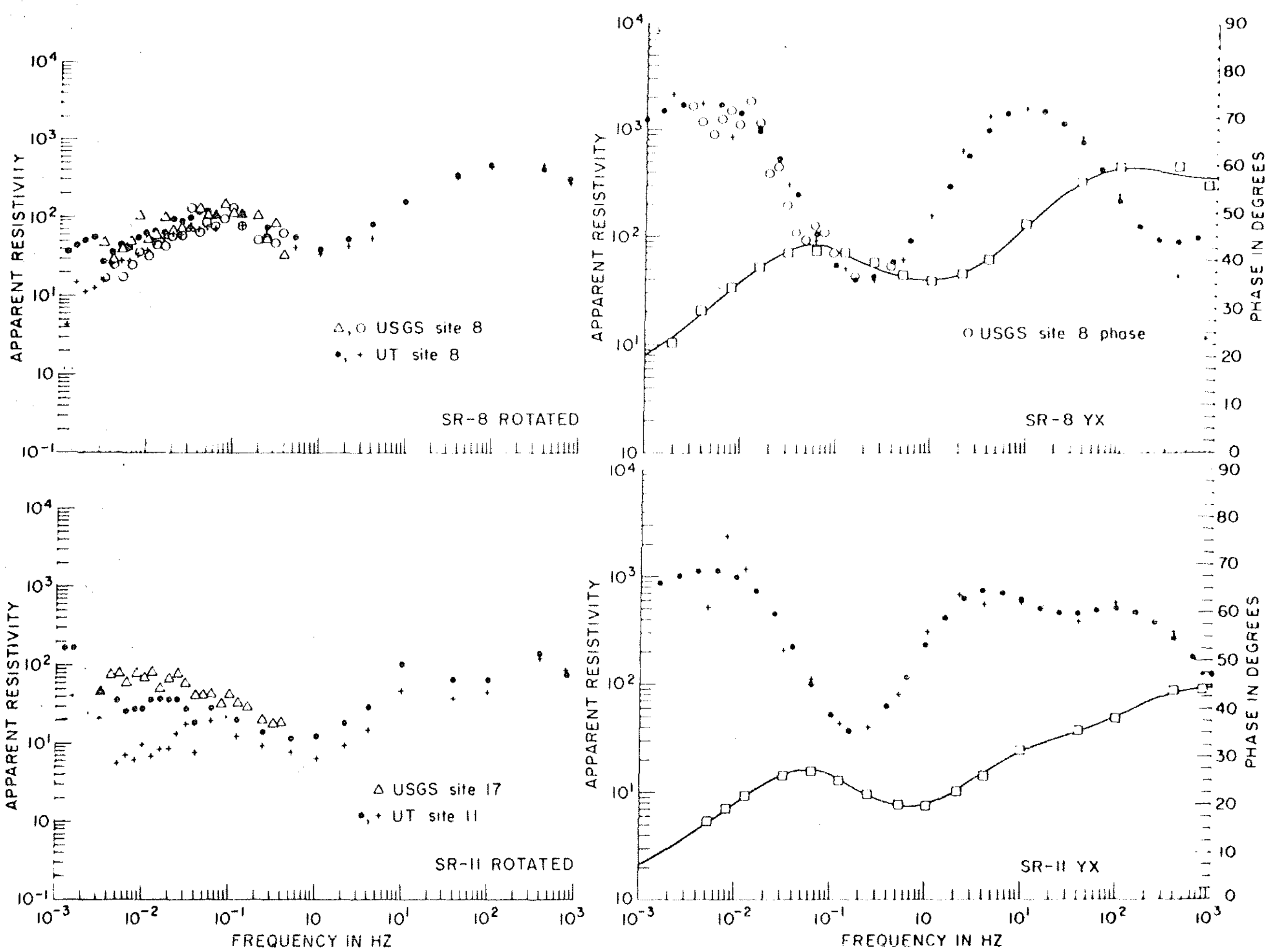

Fig. 4. MT data from UT sites 8 and 11 with data from USGS site 8 plotted on UT site 8 and data from USGS site 17 plotted on UT site 11. Because of problems with one electric channel, only scalar resistivities for one direction were obtained at site 17.

values at sites 2–8. Depths to the conductive layer are about 7 km at Raft River, 18–23 km in the central part of the Snake River Plain (sites 2, 4, and 8) and as little as 5 km at site 22 in Yellowstone. The Island Park sounding is anomalous in almost every respect, and resistivities appear to be greater than 100 ohm m down to depths of at least 23 km.

Data from the rotation parameters obtained in computing the impedance tensor for frequencies sensitive to the deepest conductor are shown in Figure 10. The line through the station location denotes the strike direction of the interpreted two-dimensional character of the data, and the small arrows point to the conductive side of the two-dimensional geometry. For simple structure on the surface of the deep conductor the conductive side is the side where the conductor is closest to the surface. At site 2 the data were too one-dimensional in character for this type of interpretation to be made, and at sites 4 and 3, no vertical magnetic field data were obtained to select TE and TM modes, but the strike direction is shown. The parameters point out the existence of conductive structures beneath the central part of the Yellowstone caldera system and suggest that a conductive axis striking about 45°NE may exist in eastern Snake River Plain. The strike parameters for the Raft River sounding are influenced by about 2 km of valley fill material to the east of the sounding site and probably do not indicate two-dimensional effects on the deep conductive zone discussed above.

Causes of Low Resistivities in the Deep Crust

The principal question to be addressed in interpreting the significance of the MT cross section is the nature of the deep conductive layer with resistivities of less than 10 ohm m and in some cases less than 1 ohm m. In order to answer this question we must look at the decrease in rock resistivities to depths of 30 km from four sources: (1) increased ionic mobility with increased temperature, (2) electronic or mineral conduction, (3) partial melting, and (4) alteration.

It is well known that the resistivity of rocks at shallow depths is mainly a function of porosity, permeability, and pore fluid resistivity, the latter being dependent upon temperature. Elevated temperatures can decrease resistivities of zero pressure rocks by an order of magnitude. To illustrate the effects of temperature and pressure on pore fluids, Figure 11 is reproduced from the paper by *Hermance* [1973], who compiled data from *Quist and Marshall* [1968]. The curves show the relationship of electrical conductivity to depth and temperature for lithostatic and hydrostatic conditions and for geothermal gradients of 60° and 120°C/km. At shallow depths the electrical conductivity increases with temperature because the pore fluid viscosity is decreasing, but ionic association decreases conductivity below depths of about 2 and 5 km for the two gradients.

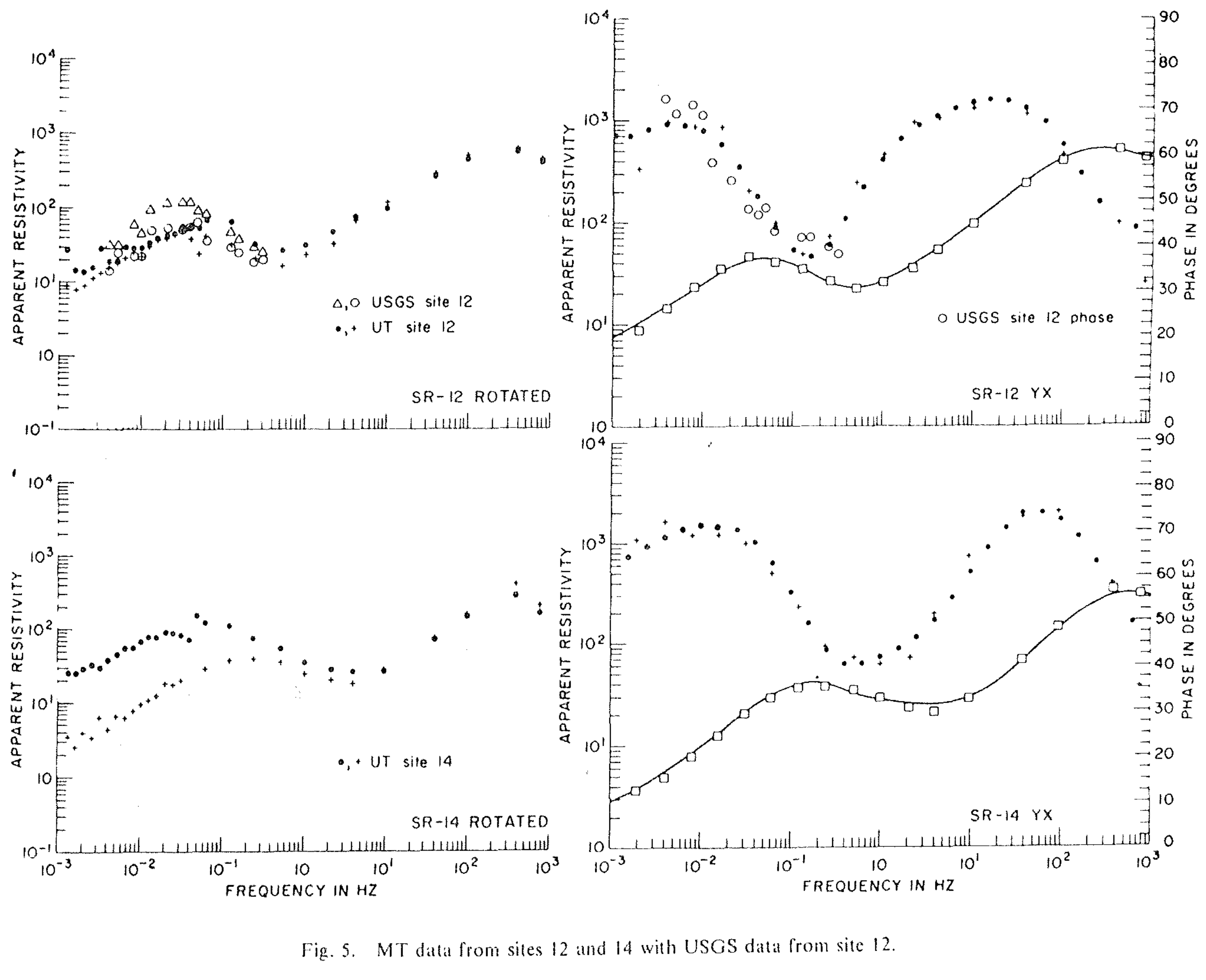

Fig. 5. MT data from sites 12 and 14 with USGS data from site 12.

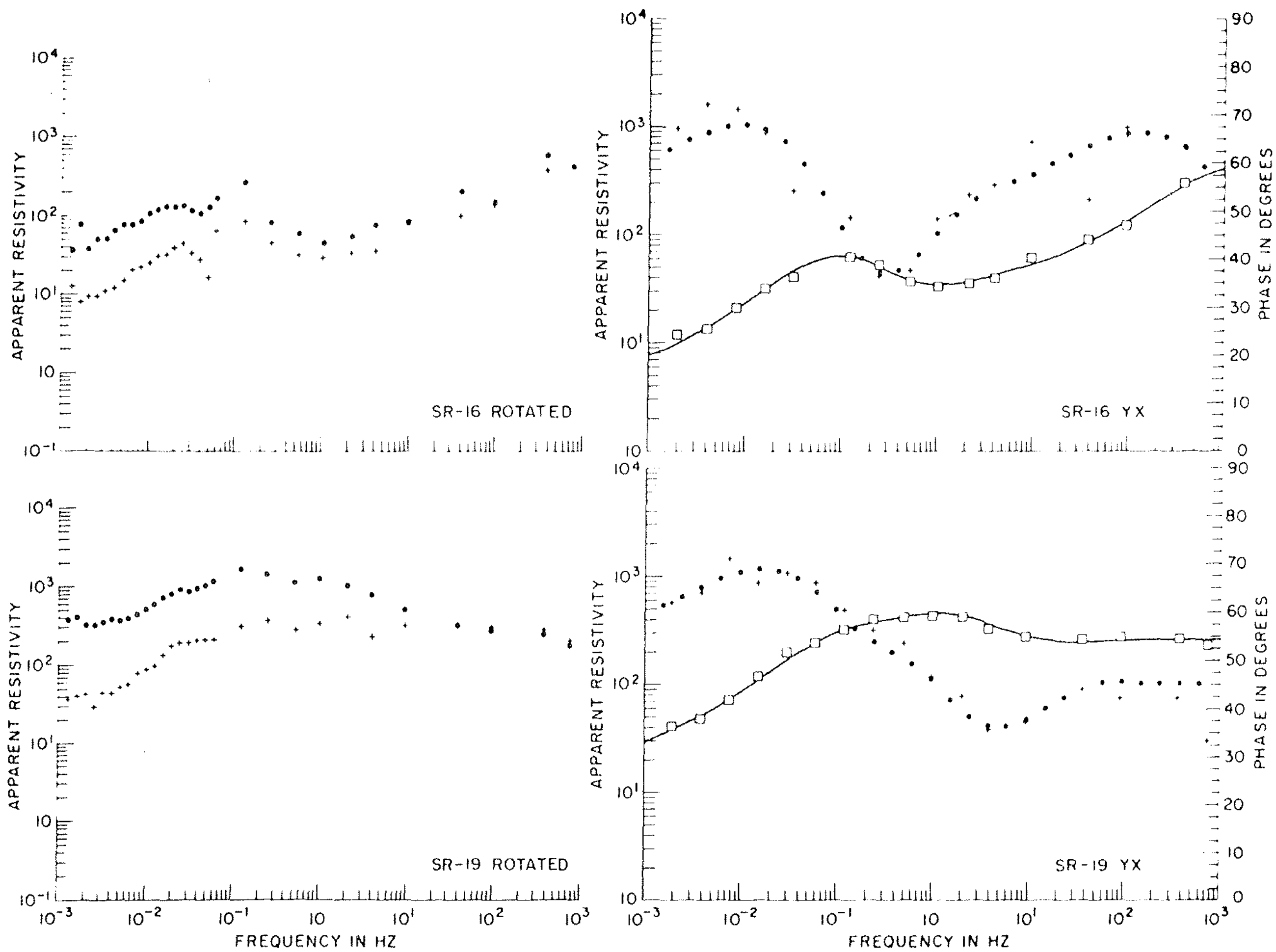

Fig. 6. MT data from sites 16 and 19.

Mineral or electronic conduction through semiconducting minerals in a rock is a function of temperature, and the lines in Figure 12 show the limits for dependence of mineral conduction upon temperature between which most measurements on dry silicate rocks fall (reproduced from the paper by *Brace* [1971]). It is obvious that mineral conduction alone is not the significant cause of low resistivities in the conductive zone in Figure 9, because resistivities of 10 ohm m are achieved only with temperatures in excess of 1000°C. Undoubtedly, mineral conduction does play a role in reducing resistivities but probably is not the major cause of the low resistivities observed in this study.

One of the main contributing factors to lowered resistivities in this study may be the partial melting of rock components. *Wyllie* [1971] has surveyed experimental pressure-temperature data on melting in the earth's crust and upper mantle. Figure 13 [from *Wyllie*, 1971] compares curves for the beginning of melting of major rock types in the presence of excess water. The granite curve represents the minimum temperature for the occurrence of melting in the crust and mantle, although traces of interstitial liquid may be produced at lower temperatures in the presence of some pore fluids. Many different rock types in the presence of pore fluids with a wide compositional range will begin to melt within a few tens of degrees of this boundary. The requirement for water-saturated conditions is admittedly an extreme one to consider routinely, but since the problem here is not how magmas are generated but how temperature affects crustal resistivities, we must keep in mind that a very small percentage of interstitial melt can reduce resistivities by a very large amount. Wyllie shows that for a granite, interstitial melt consisting largely of quartz and feldspars can exist over a large range of temperature under nonsaturation conditions for the rock as a whole.

Wyllie states that water-saturated granite liquid produced by anatexis in the crust can exist only for a few degrees above the solidus and that it appears that the normal product of anatexis is a mush composed of crystals and water-undersaturated granite liquid. The amount of original pore fluid controls the amount of liquid generated from the granitic minerals, and thus the amount of liquid necessary to complete an electrical path network can be directly related to the amount of original pore fluid and temperature-pressure curves. These types of considerations are very important in relating highly conductive parts of the earth's crust to low seismic velocity zones, since a very small amount of interstitial melt can significantly increase conductivities, lower P wave velocities, and cause S wave attenuation. These effects can be the direct result of having very small amounts of pore fluids in the original rocks and temperatures of 600°C or higher at depths of about 10 km.

An additional factor which must be considered in studying the relationship of high crustal conductivities to temperature is

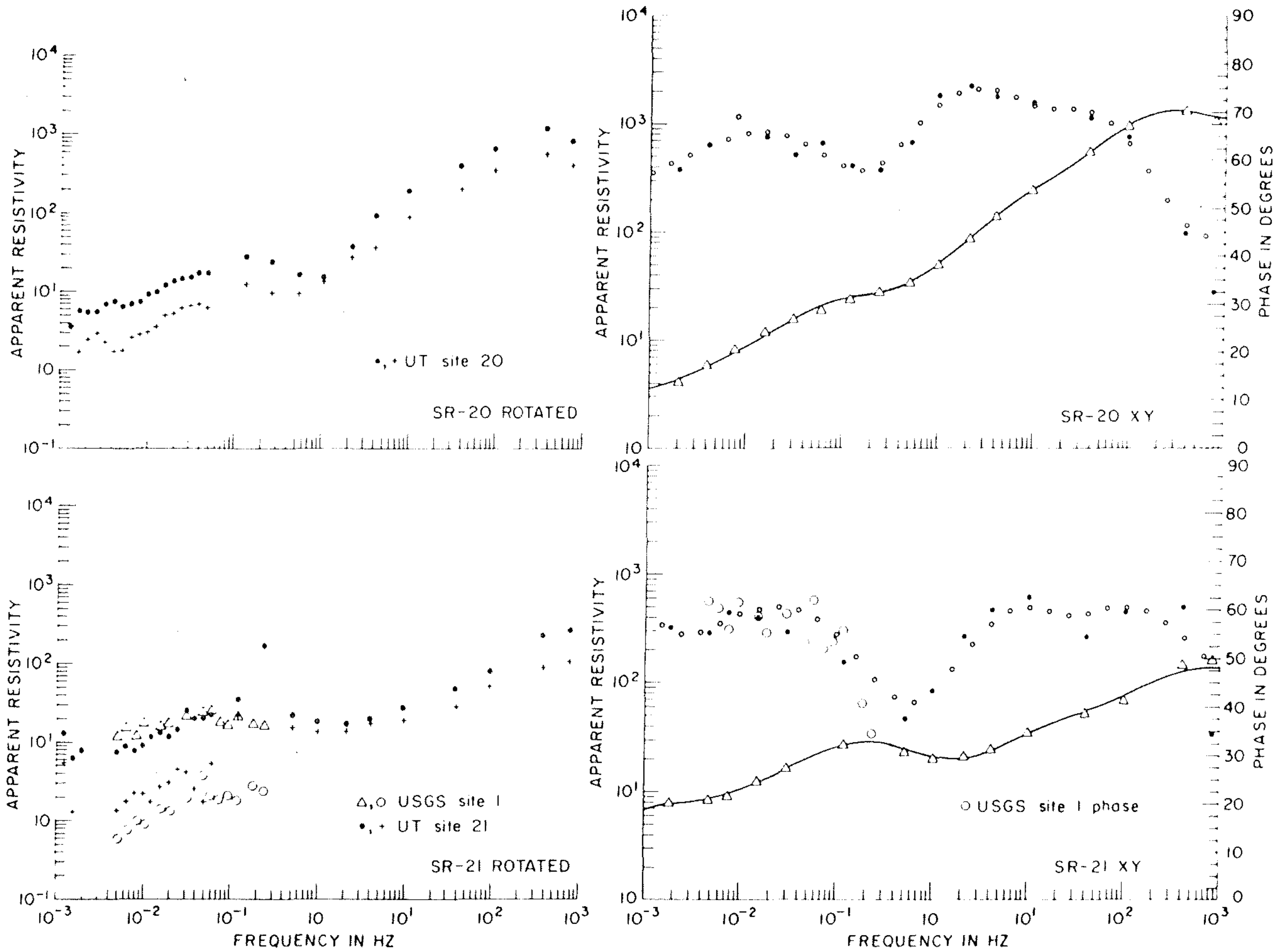

Fig. 7. MT data from sites 20 and 21 with data from USGS site 1 plotted on site 21 data.

the effect of alteration. Alteration products lining pore walls can significantly lower resistivities and control the movement of pore fluids and vapors. Recent data from experiments by *Zobacki* [1975] on the permeability of hot granite provide enlightening results regarding the complicating factor of alteration processes on the movement of pore fluids. The permeability of granite was studied at a confining pressure of 500 bars (corresponding to a depth of about 2 km), a water injection pressure of 300 bars, a differential stress to 3500 bars, and a temperature of 400°C. In all the experiments the permeability of the rock decreased from an initial value of about 5 $\times$ 10^{-6} darcys to about 0.1 $\times$ 10^{-6} darcys in the first 10 hours and to about 0.01 $\times$ 10^{-6} darcys after 10 days. In some cases the flow of water ceased altogether. The most likely explanation for this phenomenon is that alteration minerals formed during the experiment restricted the flow of water through the cracks and channels in the rock. The significance of these findings to our study is that for a given amount of pore water in the original crustal rocks at depths of interest to us (5–30 km) which have undergone a heating cycle, the pore fluids will be localized by the self-sealing effects of the rapid alteration process, and more effective local melting can occur. The effects of the rapid alteration, which over geologic time means that a hot wet granite will become more highly conductive, will add to the effects of interstitial melt and electronic conduction to provide extremely low resistivities. This total effect is substantiated by the only extensive measurements of the electrical properties in a hot wet pressurized granite system by *Lebedev and Khitarov* [1964]. Data from their study are shown in Figure 14 by the solid curves; superimposed on these data is the granite solidus curve from Figure 13. The break in the curves at the solidus is obvious, but the significant aspect of the data is the very low resistivities occurring well to the right of the solidus.

We have plotted a conservative estimate of the combined error of the depth and resistivity parameters from the MT models in Figure 13 to show where the MT data fall in relation to the sample data in order to bracket possible crustal temperatures in the survey area. It is not possible to estimate temperatures at depth accurately from the MT data by using data such as those of Figure 14 because of the unknown factors of amount of water and alteration products. However, on the basis of such data plots as the plot of the MT data in Figure 14 one might be tempted to conclude that the temperature range for the MT sites at the depth of the conductive zone is from 200°C to 800°C. This would require a great deal of structure on the isotherms, particularly in the region from Island Park to Yellowstone. This does not seem likely, and other models should be considered with mineralogical or pore fluid variations as controlling factors for resistivity.

The main cause of the large variations in the depth to the conductive layer is probably the effect of moisture content and alteration products on amounts of saturated melt and ionic mobility. Thus where the conductive zone is depressed, as at sites 2–19, water and other pore fluids and possibly alteration products are not as extensive as they are at the other sites. The reason for lower percentages of remaining pore fluids and/or alteration products, but especially pore fluids, may be related to the history of the crust. We assume that the crust has been stretched and thinned over most of the area of the MT profile, with the aid of high temperatures to provide plastic behavior. In some areas, however, the crust has been fractured quite extensively, and mantle-derived magmas have reached the surface. Also anatexis of parts of the continental crust has generated magma bodies which have erupted to the surface, as they have in the Island Park–Yellowstone area. In either instance the rising magmas may have purged water from the crustal rocks, and even though they may now have reached thermal equilibrium, the loss of pore water may have made them more resistive.

A more complicated model compatible with our MT data from the eastern Snake River Plain may be considered as an alternative. We refer to a model derived for the western plain to explain seismic [*Hill and Pakiser*, 1966] and gravity data [*Mabey*, 1975]. Mabey has compiled a gravity model for the western part of the Snake River Plain based upon the seismic refraction profile of Hill and Pakiser and his gravity data. A large amplitude gravity high is coincident with the topographic low of the Snake River Plain. *Mabey* [1975] calculates that the plain is in isostatic equilibrium and suggests that for a feature as narrow as the western Snake River Plain to be approximately in isostatic equilibrium, the compensating mass is likely to be partly within the crust. The seismic data interpretations by *Hill and Pakiser* [1966] suggest that the normal upper crust is either very thin or absent under the axis of the western plain and that the lower crust with a velocity of 6.7 km/s extends to about 42 km below the surface and is underlain by a 7.9-km/s mantle. Mabey's gravity model for the western Snake River Plain has an upper crust of granitic composition with a density of 2.65 g/cm^3 and a lower crust of more basic composition with a density of 3.0 g/cm^3. Mabey correlates the upper crust of low density and granitic composition with Hill and Pakiser's seismic layer having a velocity of 6.0 km/s and the lower crustal unit of density 3.0 g/cm^3 with Hill and Pakiser's velocity layer of 6.7 km/s. The density of the lower crustal unit may be close to that of the upper mantle, which is interpreted to be at a depth of 40 km beneath the Snake River Plain on the seismic profile, 10 km greater than the depth south of the plain on the same profile. Even though there are no similar seismic data available for the eastern Snake River Plain, we believe that compensation of the upper mantle and lower crust to stretching and thinning processes may be similar to that postulated for the western part of the plain. In view of this possibility we have constructed an alternate crustal model (along the lines of the Hill and Pakiser and Mabey models) which attempts to rationalize some of the conductivity phenomena. This model is shown in Figure 15 with what we propose as a possible isotherm distribution. Establishing the isothermal dis-

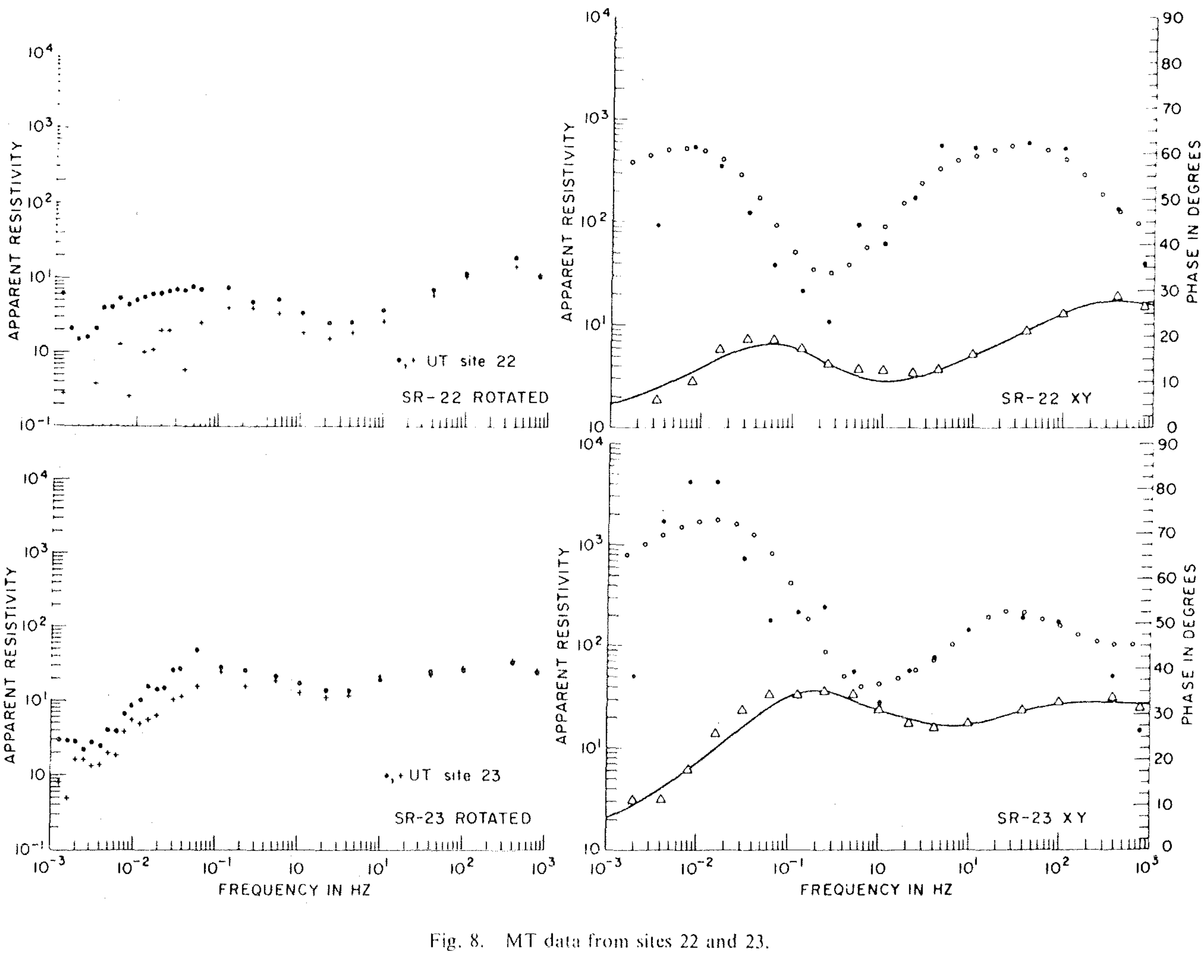

Fig. 8. MT data from sites 22 and 23.

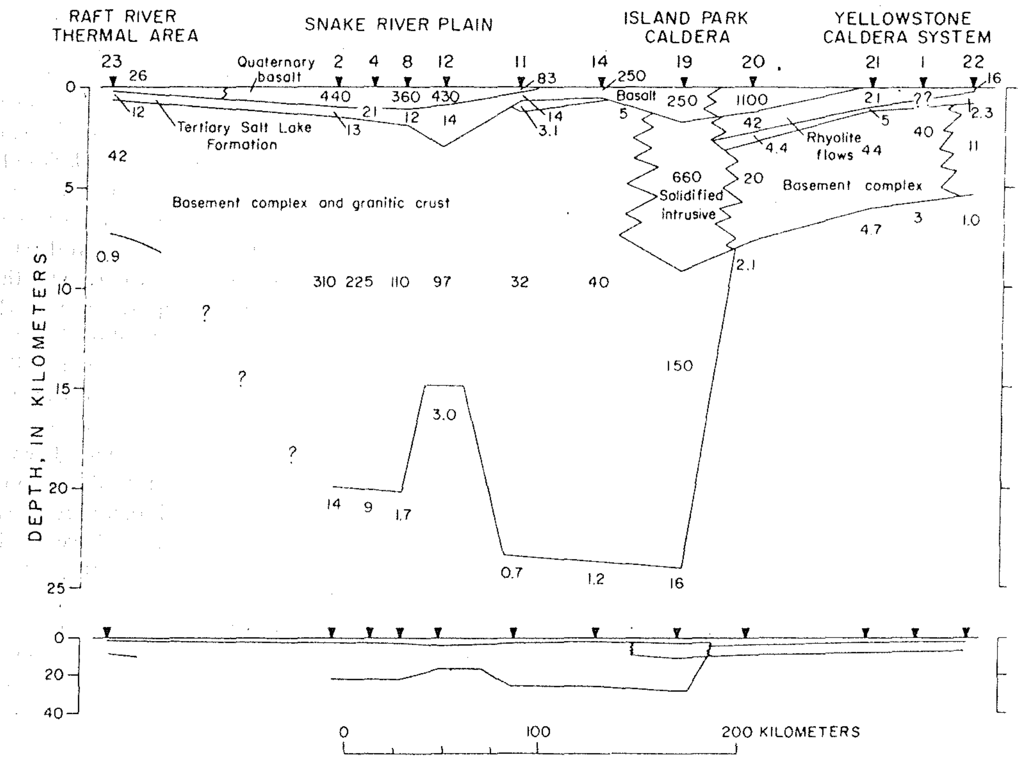

Fig. 9. Geoelectrical cross section compiled from MT one-dimensional models. Numbers in model layers are interpreted resistivites in ohm meters. Where a relationship appears to exist between an electrical layer and a geologic unit, the unit is labeled. Vertical exaggeration is 10 to 1 for the upper cross section and 1 to 1 for the lower cross section.

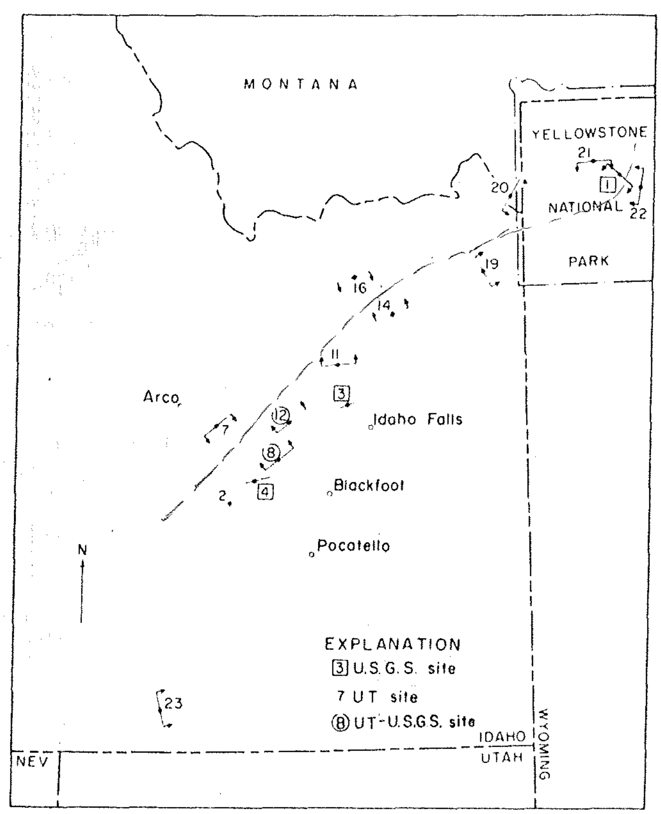

Fig. 10. Two-dimensional structural parameters obtained by rotating the impedance tensor. The line through the station location denotes the strike of the assumed two-dimensionality, and the small arrows point to the conductive side of the structure.

tribution with reference to deep electrical measurements would be much simpler if more laboratory studies on a variety of rocks were available, but since they are not, the isothermal distribution of Figure 15 must be considered as being very speculative. Conductivity effects in granites for one set of samples have been illustrated in Figure 14. However, granitic rocks under crustal conditions may be considerably more con-

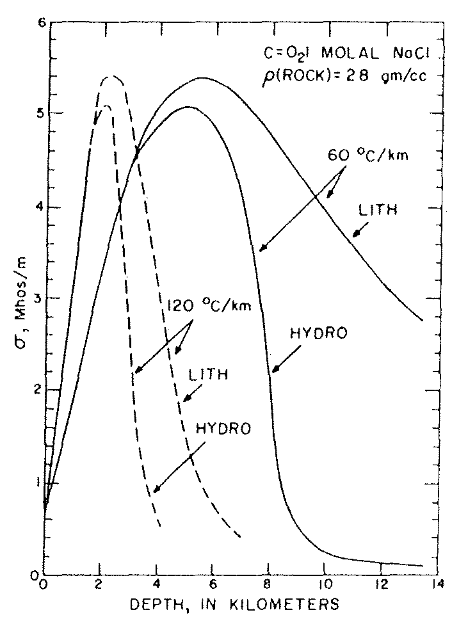

Fig. 11. Pore fluid conductivity as a function of depth under lithostatic and hydrostatic conditions for geothermal gradients of 60° and 120°C/km. The electrolyte has an equivalent NaCl concentration of 0.1 molal.

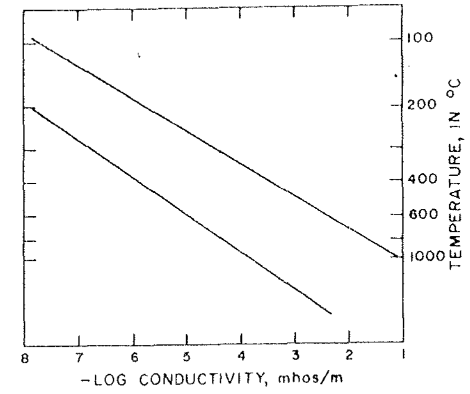

Fig. 12. Minimum and maximum boundary lines for electronic conduction effects in a variety of rock samples [from *Brace*, 1971].

ductive than the laboratory samples because of the great lengths of time available for alteration processes to take place and for the corrosive effects of water above the critical point to take effect. These processes have a relatively short time constant, as the previously mentioned granite permeability studies show, but in any event we would expect the crustal rocks to be more conductive than the laboratory samples. With these assumptions in mind we used the 500°C isotherm as the minimum temperature for large changes in conductivity of the granitic crust to occur when we were compiling Figure 14. The water content of the lower crustal material of more basic constituency is assumed to be lower than that of the upper crust, and thus we consider that the 700°C isotherm may be closer to the minimum temperature at which large changes in conductivity occur for the lower crust. Most of the model of Figure 14 is built from these two main assumptions. Island Park must still be accounted for, and we again take the position that moisture has been purged from the crust beneath Island Park and that there may be mineralogical differences as well. Granitic magmas may be present at depths of 5–20 km where we indicate temperatures above 650°C (refer to Figure 12, Wyllie's solidus curves) in the water present upper crust.

We have used thicknesses of the granitic upper crust obtained from the seismic and gravity models for the western Snake River Plain. The MT data cannot provide any information on the relative thicknesses of the postulated upper and lower crustal layers. The only constraint provided by the electrical data is tied to our assumption that the 500°C isotherm

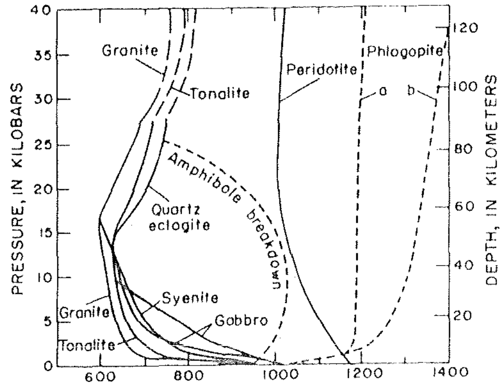

Fig. 13. Solidus curves for a variety of rock types [from *Wyllie*, 1971].

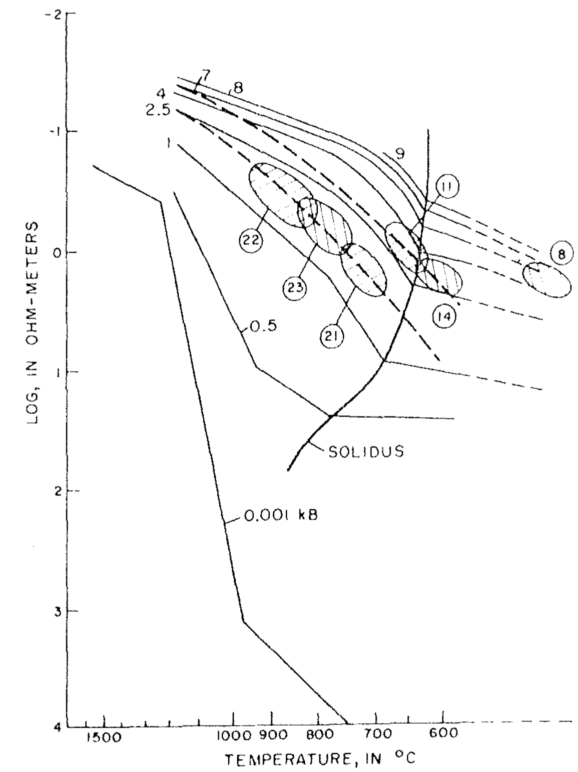

Fig. 14. Electrical resistivity measurements on a hot wet pressurized granite [from *Lebedev and Khitarov*, 1964]. The vertical axis is resistivity in log ohm meters, and the horizontal axis is temperature in log spacing. The parametric curves are for various water vapor pressures in kilobars. A solidus curve for granite [from *Wyllie*, 1971] is shown crossing the parametric curves. The cross-hatched ellipses represent the uncertainty area for the resistivity-depth parameters from several MT soundings, designated by the circled numbers. We have roughly extrapolated the data outside the original data area to plot MT data from site 8.

defines a major break in conductivity in the upper crust, whereas the 700°C isotherm defines a major break in the lower crust. The same general isothermal distribution is compatible with a model incorporating variable water content in a granitic crust to explain the conductive surface undulations. The model of Figure 14 is merely an attempt to incorporate the idea of a stretched and thinned crust and to indicate what effect a dryer basaltic lower crust would have on the resistivities.

To illustrate that our estimates of temperature from the MT data are reasonable, we show in Figure 16 four representative 'continuous' MT models plotted along with theoretical resistivity-depth curves computed by *Olhoeft* [1976]. The theoretical curves are an attempt to include most of the parameters affecting resistivity, including changes in porosity with depth, changes in solution activity with pressure and temperature, changes in pore fluid resistivity with temperature and pressure, solid conduction, ionic conduction, and changes in the critical point of water with temperature and pressure, but neglecting the effect of alteration. Curve A is for a temperature gradient of 60°C/km, a pressure gradient of 250 bars/km, and increasing salt saturation with temperature; curve B is for the same conditions as curve A, except that the gradient is 120°C/km; curve C is for a temperature gradient of 120°C/km, a pressure gradient of 250 bars/km, and increasing salt saturation with temperature, and the critical point of water is dependent upon salt concentration. The curves were computed by assuming a basaltic or granitic rock where water accessible porosity is 4% at the surface but changes with depth [after *Brace*, 1971]. We

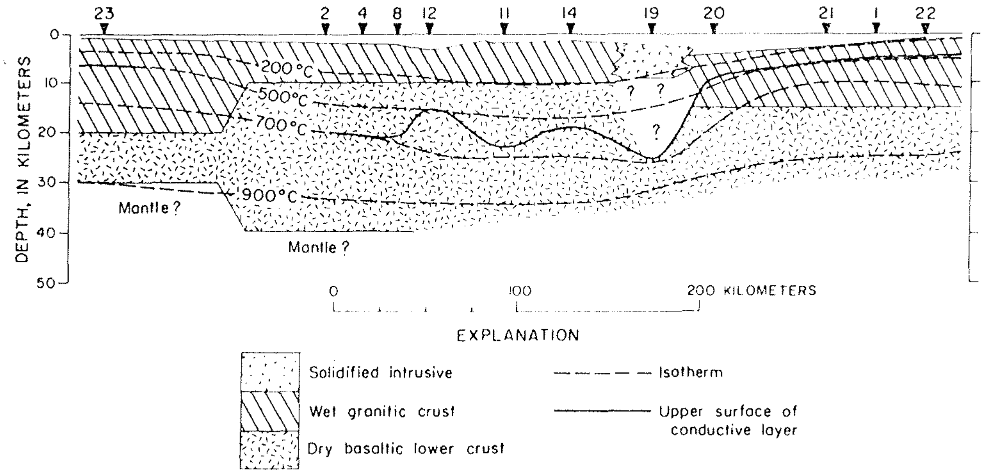

Fig. 15. Isothermal and geoelectrical model designed for compatibility with the seismic model of *Hill and Pakiser* [1966] and the gravity model of *Mabey* [1975].

assume a mean surface value of 100 ohm m for such a rock with large amounts of alteration. This value was taken from the average for the resistive layer on the Snake River Plain sites and the Raft River site and from past experience with highly altered basalts and granites. Shown plotted in Figure 16 are data from the 'continuous' inversions for sites 8, 11, 22, and 23. The MT data cannot be compared to the theoretical curves for the region above about 2 km, the average depth to the basement complex and upper crustal layer of Figures 8 and 14. Below this depth, however, the data for sites 11, 22, and 23 appear to agree best with the assumptions made for theoretical curve C. Geothermal gradients for each of the sites taken from the model of Figure 15 are shown, and it appears that gradients derived from the assumptions of this alternative model are reasonable for the crustal situation modeled in the theoretical curves. The only heat flow measurements available for any of the sites for which data are shown in Figure 14 come from the Raft River thermal area, near site 23. Several thermal gradient measurements made at a depth of 1 km or less in the Raft River area provide an average estimate of 50°C/km for the geothermal gradient (B. Diment, oral communication, 1976). The temperature at the bottom of the deepest hole drilled in Raft River (about 2 km) was found to be 145°–150°C, giving a gradient of 75°C/km; however, evidence exists that part of the system is convecting near the bottom of the hole, and thus the actual conductive gradient is smaller. These values are not too different from our estimate of 69°C/km from the MT data (see Figure 16). Other theoretical curves can be constructed that will look quite different from those of Figure 16, but we propose that the thermal-tectonic model portrayed in Figure 15 is a likely candidate for the true situation in the eastern Snake River Plain–Yellowstone region.

Yellowstone Area

Yellowstone represents an obvious active thermal anomaly with an extent possibly deep into the mantle [*Eaton et al.*, 1975] and thus the reason for which we show shallower isotherms, with the support of the MT interpretations, under Yellowstone. Our results relate to previous work in several respects. In the paper by *Eaton et al.* [1975], results of gravity studies suggest that a magma chamber exists in the northeast corner of the Yellowstone caldera system, centered approximately 10–15 km northeast of MT site 1. We do not have an MT sounding in the middle of the gravity anomaly, but the structural parameters shown in Figure 10 show that the most conductive region of the Yellowstone caldera system is centered more in the central or possibly the western part of the system. This finding seems to correlate with the teleseismic *P* wave residual anomaly discovered by H. M. Iyer and described by *Eaton et al.* [1975], which is centered in the central and western parts of the caldera. In addition, a teleseismic wave attenuation anomaly is centered near the middle of the caldera system. Local seismicity in the Yellowstone area is quite high, as described by Eaton, but much reduced inside the caldera system itself. Focal depths are generally less than 15 km outside the caldera, but within the northwestern part of the caldera the maximum focal depth is only 5 km [*Smith et al.*, 1974]. These depths correspond quite well to the depth to the conductive zone from the MT cross section, and it is not surprising that the zone where we postulate intense alteration and partial melting is a zone that does not support earthquakes. The depth of 5–7 km for the conductive layer in Yellowstone also corresponds to a depth of about 5–6 km to the Curie isotherm estimated by *Bhattacharyya and Leu* [1975]. The Curie isotherm is generally quoted to be 500°–600°C, and this seems to fit with the isotherms derived from the electrical models of this study.

Conclusions

The conductive zone at shallow depths in the crust discov-

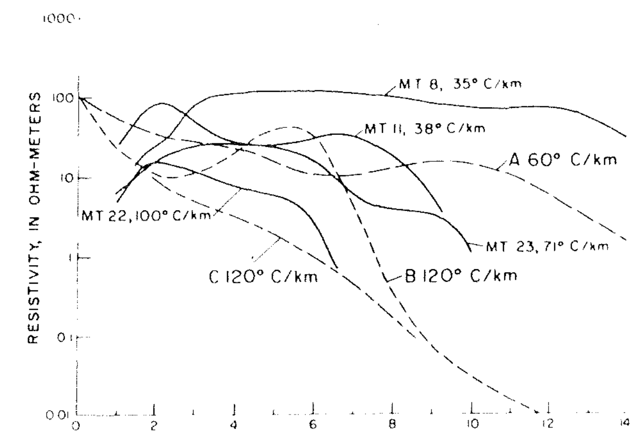

Fig. 16. Theoretical resistivity-depth curves by *Olhoeft* [1976] showing various assumptions A, B, and C (see text for explanation); also plotted are 'continuous' inversions for MT sites 8, 11, 22, and 23.

ered in this MT study is very probably caused by elevated temperatures. Actual temperatures cannot be estimated accurately from the MT interpretations because of the lack of good laboratory measurements on crustal rocks with all variables under control. Our portrayal of the isotherms in Figure 15 is supported by several lines of evidence but by few good experimental data.

The MT sounding in the Raft River thermal area indicates that near-surface geothermal reservoirs probably have their origin in an abnormally hot crust and need not be explained by deep circulation of groundwater in an area of normal heat flow, as has been proposed for this area (D. R. Mabey, oral communication, 1976). The MT soundings in Yellowstone may be interpreted to mean that the center of current magmatic activity is in the central or western part of the caldera system as outlined by seismic delay and attenuation studies. The depths to the conductive zone in Yellowstone determined by the MT modeling correspond to Curie point depths and to maximum focal point depths. The MT model cross section shows a dramatic decrease in depth to the conductive zone from the eastern Snake River Plain to Yellowstone, near Island Park. A model consistent with seismic and gravity interpretations for the western Snake River Plain has been offered as a possible attempt to explain the variation in depths to the conductive zone.

The conductive zone in the crust found in this survey may be

TABLE 1. One-Dimensional Model Data for Snake River Plain, Idaho, 1975

			Model Parameters			
Site	E	Φ', deg	Layer	ρ, ohm m	T, km	D, km
SR-2	XY	indeterminate	1	440	0.9	0.9
			2	13	0.5	1.4
			3	310	18.4	19.8
			4	14		
SR-7	XY	−46	1	250	0.4	0.4
			2	17	2.4	2.8
			3	600	11.8	14.6
			4	5.7		
SR-8	YX	−40	1	360	1.0	1.0
			2	12	0.7	1.7
			3	110	18.4	20.1
			4	1.7		
SR-11	XY	174	1	106	0.4	0.4
			2	10	2.0	2.4
			3	76	21.0	23.4
			4	1.2		
SR-12	YX	−39	1	430	0.8	0.8
			2	14	2.0	2.8
			3	97	11.9	14.7
			4	3.0		
SR-14	XY	97	1	231	0.4	0.4
			2	6.7	0.3	0.7
			3	160	19.2	19.9
			4	1.2		
SR-16	YX	161	1	360	0.3	0.3
			2	30	2.5	2.8
			3	104	10.4	13.2
			4	3.5		
SR-19	YX	59	1	250	1.7	1.7
			2	660	7.4	9.1
			3	150	14.8	23.9
			4	16		
SR-20	XY	−62	1	1100	1.2	1.2
			2	42	1.0	2.2
			3	4.4	0.5	2.7
			4	20	4.8	7.5
			5	2.1		
SR-21	XY	175	1	120	0.2	0.2
			2	21	0.6	0.8
			3	5.0	0.2	1.0
			4	44	4.8	5.8
			5	4.7		
SR-22	XY	96	1	16	0.1	0.1
			2	2.3	0.6	0.7
			3	11	4.5	5.2
			4	1.0		
SR-23	XY	−103	1	26	0.2	0.2
			2	12	0.4	0.6
			3	42	6.6	7.2
			4	0.9		

compared with similar findings in the Carson Sink area of Nevada where an MT study [*Stanley et al.*, 1976] revealed a conductive zone at depths of 4–7 km with resistivities of less than 1 ohm m. Both of these areas very probably have underlying hot crust, and in particular the MT study in the Carson Sink was done where seismic refraction studies found that the crust is only 22 km thick [*Pakiser and Hill*, 1963]. These findings should have a great deal of impact on geothermal exploration and on the estimation of the total geothermal resources of the western United States. The power of the MT method for mapping regional thermal anomalies has been demonstrated by both surveys, and the technique should play a major role in determining the total geothermal resource.

Acknowledgments. Participation by the University of Texas at Austin Geomagnetics Laboratory in this study was funded by National Science Foundation and USGS grants. The investigators wish to thank the Bureau of Land Management and the Yellowstone National Park administrators for allowing access to many of the MT sites. The cryogenic magnetometer used as part of the USGS MT system was developed by Nolan Frederick and Jim Zimmerman of the National Bureau of Standards, Boulder, Colorado. We wish to thank G. R. Olhoeft of USGS for many helpful discussions on rock properties and for allowing us to use the theoretical curves of Figure 16.

REFERENCES

Anderson, A. L., Lava Creek vents, Butte County, Idaho, *Northwest Sci.*, *3*, 13–19, 1929.

Becher, W. D., and C. B. Sharpe, A synthesis approach to magnetotelluric exploration, *Radio Sci.*, *4*, 1089–1094, 1969.

Bhattacharyya, B. K., and L.-K. Leu, Analysis of magnetic anomalies over Yellowstone National Park: Mapping of Curie point isothermal surface for geothermal reconnaissance, *J. Geophys. Res.*, *80*(32), 4461–4465, 1975.

Bonini, W. E., Gravity anomalies in Idaho, *Rep. 132*, Idaho Bur. of Mines and Geol., Boise, 1963.

Bostick, F. X., Jr., and H. W. Smith, Investigation of large scale inhomogeneities in the earth by the magnetotelluric method, *Proc. Inst. Radio Eng.*, *50*, 2339–2346, 1962.

Brace, W. F., Resistivity of saturated crustal rocks to 40 km based on laboratory measurements, in *The Structure and Physical Properties of the Earth's Crust*, vol. 14, *Geophys. Monogr.*, edited by J. G. Heacock, pp. 243–255, AGU, Washington, D. C., 1971.

Bullard, F. M., Volcanic history of the Great Rift, Craters of the Moon National Monument, South Central Idaho (abstract), *Geol. Soc. Amer. Bull.*, *2*, 273–274, 1971.

Cagnaird, L., Basic theory of the magnetotelluric method of geophysical prospecting, *Geophysics*, *18*, 605–635, 1953.

Cantwell, T., Detection and analysis of low frequency magnetotelluric data, Ph.D. thesis, Dep. of Geol. and Geophys., Mass. Inst. of Technol., Cambridge, 1960.

Christiansen, R. L., and H. R. Blank, Jr., Volcanic stratigraphy of the Quaternary rhyolite plateau in Yellowstone National Park, *U.S. Geol. Surv. Prof. Pap.*, *729-B*, 1–18, 1972.

Eaton, G. P., R. L. Christiansen, H. M. Iyer, A. M. Pitt, D. R. Mabey, H. R. Blank, Jr., I. Zietz, and M. E. Gettings, Magma beneath the Yellowstone National Park, *Science*, *188*, 787–796, 1975.

Greenfield, R. J., and L. S. Turnbull, Jr., Monte Carlo inversion of magnetotelluric data (abstract), *Eos Trans. AGU*, *51*, 426, 1970.

Hermance, J. F., An electrical model for the sub-Icelandic crust, *Geophysics*, *38*(1), 3, 1973.

Hill, D. P., Gravity and crustal structure in the western Snake River Plain, Idaho, *J. Geophys. Res.*, *68*(20), 5807–5819, 1963.

Hill, D. P., and L. C. Pakiser, Crustal structure between the Nevada Test Site and Boise, Idaho, from seismic-refraction measurements, in *The Earth Beneath the Continents*, vol. 10, *Geophys. Monogr.*, edited by J. S. Steinhart and T. J. Smith, pp. 391–419, AGU, Washington, D. C., 1966.

Iyer, H. M., Seismic noise studies in Yellowstone National Park, *Nature*, *253*, 425, 1975.

Jackson, D. B., Report on direct current soundings over a geothermal prospect in the Bruneau-Grandview area, Idaho, *Open File Rep. 74*, U.S. Geol. Surv., Denver, Colo., 1974.

Johnson, I. M., and D. E. Smylie, An inverse theory for the calculation of the electrical conductivity of the lower mantle, *Geophys. J. Roy. Astron. Soc.*, *22*, 41–53, 1970.

Laird, E. E., and F. X. Bostick, Jr., One-dimensional magnetotelluric inversion techniques, *Tech. Rep. 101*, Elec. Eng. Res. Lab., Univ. of Tex., Austin, 1970.

Leary, F., and R. A. Phinney, A magnetotelluric traverse across the Yellowstone region, *Geophys. Res. Lett.*, *1*(6), 265, 1975.

Lebedev, E. B., and N. I. Khitarov, Dependence of the beginning of melting of granite and the electrical conductivity of its melt on high water vapor pressure (in Russian), *Geokhimiya*, no. 3, 195–201, 1964.

Long, C. L., J. E. O'Donnell, and B. D. Smith, Geophysical studies in Island Park, Eastern Idaho, *J. Res. U.S. Geol. Surv.*, in press, 1977.

Mabey, D. R., Interpretation of a gravity profile across the western Snake River Plain, Idaho, *Geology*, *4*(1), 53–55, 1975.

Malde, H. E., Fault zone along northern boundary of western Snake River Plain, Idaho, *Science*, *130*, 272, 1959.

McIntyre, D. H., Cenozoic geology of the Reynolds Creek experimental watershed, Owyhee County, Idaho, *Rep. 151*, 155 pp., Idaho Bur. of Mines and Geol., Boise, 1972.

Olhoeft, G. R., Electrical properties of basalt (abstract), *Eos Trans. AGU*, *57*(4), 236, 1976.

Oppenheim, A. B., and R. W. Schafer, *Digital Signal Processing*, 458 pp., John Wiley, New York, 1975.

Otnes, R. K., and L. Enochson, *Digital Time Series Analysis*, 467 pp., John Wiley, New York, 1972.

Pakiser, L. C., and D. P. Hill, Crustal structure in Nevada and southern Idaho from nuclear explosions, *J. Geophys. Res.*, *68*(20), 5757–5766, 1963.

Patrick, F. W., and F. X. Bostick, Jr., Magnetotelluric modeling techniques, *Tech. Rep. 59*, Elec. Eng. Res. Lab., Univ. of Tex., Austin, 1969.

Quist, A. S., and W. L. Marshall, Electrical conductances of aqueous sodium chloride solutions from 0° to 800°C and at pressures to 4,000 bars, *J. Phys. Chem.*, *72*, 684–703, 1968.

Sims, W. E., and F. X. Bostick, Jr., Methods of magnetotelluric analysis, *Tech. Rep. 58*, Elec. Eng. Res. Lab., Univ. of Tex., Austin, 1969.

Smith, R. B., R. T. Shuey, R. O. Friedline, R. M. Otis, and L. B. Alley, Yellowstone hot spot: New magnetic and seismic evidence, *Geology*, *2*, 451, 1974.

Stanley, W. D., D. B. Jackson, and A. A. R. Zohdy, Deep electrical investigations in the Long Valley geothermal area, California, *J. Geophys. Res.*, *81*(5), 810, 1976.

Swift, C. M., Jr., A magnetotelluric investigation of an electrical conductivity anomaly in the southwestern United States, Ph.D. thesis, Geophys. Dep., Mass. Inst. of Technol., Cambridge, 1967.

Williams, P. L., D. R. Mabey, A. A. R. Zohdy, H. Ackermann, D. B. Hoover, K. L. Pierce, and S. S. Oriel, Geology and geophysics of the southern Raft River Valley geothermal area, Idaho, USA, *Open File Rep. 75-322*, U.S. Geol. Surv., Denver, Colo., 1975.

Word, D. R., H. W. Smith, and F. X. Bostick, Jr., An investigation of the magnetotelluric tensor impedance method, *Tech. Rep. 82*, Elec. Eng. Res. Lab., Univ. of Tex., Austin, 1970.

Wu, F. T., The inverse problem of magnetotelluric sounding, *Geophysics*, *33*, 972–979, 1968.

Wyllie, P. J., Experimental limits for melting in the earth's crust and upper mantle, 14, in *The Structure and Physical Properties of the Earth's Crust*, vol. 14, *Geophys. Monogr.*, edited by J. G. Heacock, pp. 279–301, AGU, Washington, D. C., 1971.

Zobacki, M. D., High pressure deformation and fluid flow in sandstone, granite and granular materials, Ph.D thesis, Dep. of Geophys., Stanford Univ., Palo Alto, Calif., 1975.

Zohdy, A. A. R., and W. D. Stanley, Preliminary interpretation of electrical sounding curves obtained across the Snake River Plain from Blackfoot to Arco, Idaho, open file report, U.S. Geol. Surv., Denver, Colo., 1973.

Zohdy, A. A. R., L. A. Anderson, and L. J. P. Muffler, Resistivity self-potential, and induced polarization surveys of a vapor-dominated geothermal system, *Geophysics*, *38*(6), pp. 1130–1144, 1973.

(Received September 7, 1976;
revised January 31, 1977;
accepted February 2, 1977.)